

NEW PULSED ORBIT BUMP MAGNETS FOR THE FERMILAB BOOSTER SYNCHROTRON*

J.R. Lackey#, J.A. Carson, C.M. Ginsburg, H.D. Glass, D.J. Harding, V.S. Kashikhin, A. Makarov, E.J. Prebys

Fermi National Accelerator Laboratory, Batavia, IL 60510

Abstract

The beam from the Fermilab Linac is injected onto a bump in the closed orbit of the Booster Synchrotron where a carbon foil strips the electrons from the Linac's negative ion hydrogen beam. Although the Booster itself runs at 15 Hz, heat dissipation in the orbit bump magnets has been one limitation to the fraction of the cycles that can be used for beam. New 0.28 T pulsed dipole magnets have been constructed that will fit into the same space as the old ones, run at the full repetition rate of the Booster, and provide a larger bump to allow a cleaner injection orbit. The new magnets use a ferrite in the yoke rather than laminated steel.

INTRODUCTION

The present injection system for the Fermilab Booster was designed in the early 1990s and was built with stacking operations to the Fermilab P-Bar Source in mind. Operation with repetition rates higher than 20% (3 Hz) were never expected. Typical rates were on the order of 10%. Currently the Booster provides protons for MiniBooNE and NUMI, as well as the P-Bar Source and will require the capability of repetition rates to 10 Hz or more. Due to severe heating in the present magnets the operational repetition rate is limited to 7.5 Hz. New magnets have been designed which are capable of continuous operation at 15 Hz (100% duty factor). These magnets have been designed to be radiation hard. The new magnets are stronger than the present magnets by ~15%. This increase in strength will allow injection into the Booster with the injection closed orbit at the center of the horizontal aperture rather than 1 cm radially outside of center as at present. This will significantly increase the horizontal injection aperture. These magnets will be installed in the Booster during the fall shutdown 2005.

In operation the magnets see a current waveform that rises roughly linearly in 20 μ S to a plateau at about 15 kA. The current is held constant during injection of multiple turns of beam, up to 35 μ S. The current is then ramped down over 20 μ S.

CONSTRUCTION

The magnet cross section is shown in Figure 1. The major differences between the new magnet design and the old are cooling for the conductor and the use of G4, a NiZn ferrite [1], for the magnet core instead of laminated

steel. The use of ferrite provides several benefits. Construction is simplified because the stack up of precision-machined ferrite blocks is much easier than stacking and gluing many thousands of very thin steel laminations. The amount of epoxy in the vacuum is reduced. It is also not necessary to insulate the current conductor or the ferrite core.

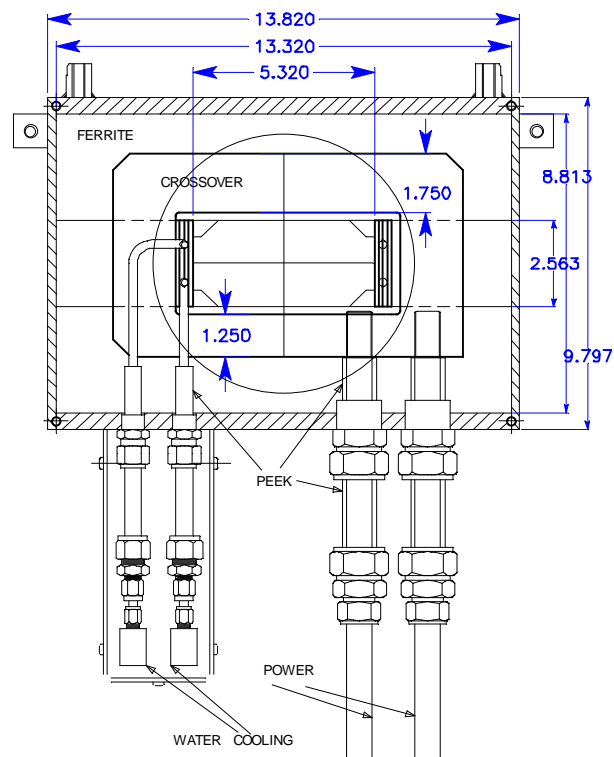


Figure 1 Magnet cross section and power and water leads. (Dimensions in inches)

Core power losses are considerably reduced and it is not necessary to actively cool the core. Any necessary core cooling is provided by direct conduction to the stainless steel skin of the magnet. It is estimated that the core loss is reduced from ~1 kW to ~200 Watts by the use of ferrite instead of laminations.

The only electrical insulation used in the magnet is at the feed-through from vacuum to atmosphere for the power and cooling water. The insulating material is PEEK [2] which has excellent radiation resistant properties. Standard double ferrule fittings provide the vacuum seal between the copper current conductors, the PEEK insulators, and the stainless steel vacuum skin. The nominal magnet parameters are listed in Table 1.

* Work supported by the United States Department of Energy under Contract No. DE-AC02-76CH03000
#lackey@fnal.gov

Table 1: Nominal Magnet Parameters

Parameter	Value	Units
$\int B_y dl$ @ 15 kA	0.1676	T-m
Ferrite length	523.3	mm
Effective length	558.5	mm
Aperture gap	65.1	mm
Aperture width	135.1	mm
Inductance	1.83	μH
Resistance	<1	m Ω

FIELD CALCULATIONS

During the magnet design the field was modeled in three dimensions at the operating frequency using Opera-3D [3]. There is a quadrupole component of the field at the lead end due to the asymmetrical configuration of the leads and their connection to the single turn coil. Figure 2 shows the main bending field B_y at $y=0$ as a function x and z .

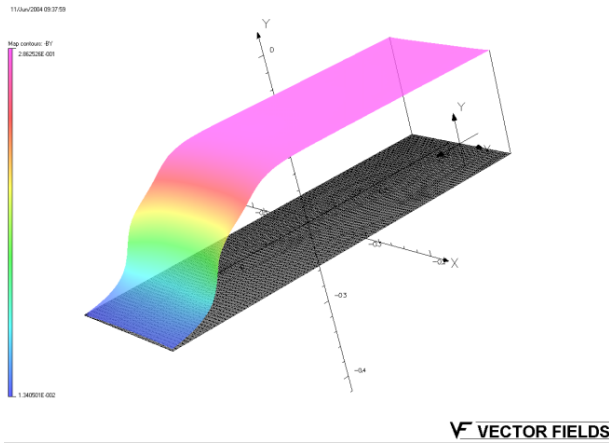


Figure 2 Calculated B_y at $y=0$ as a function of x and z through the end of the magnet.

FIELD MEASUREMENTS

DC Measurements

Magnetic measurements have been made at a low DC current, 1700 A, allowing precise determination of all field components due to geometrical effects. The primary measurement tool was a rotating tangential coil that extended through the magnet, measuring all components of the field integral. Figure 3 shows the integral of the main field, $\int B_y dl$, as a function of horizontal position, recreated from the harmonic components.

ORBD001, field shape from tangential coil

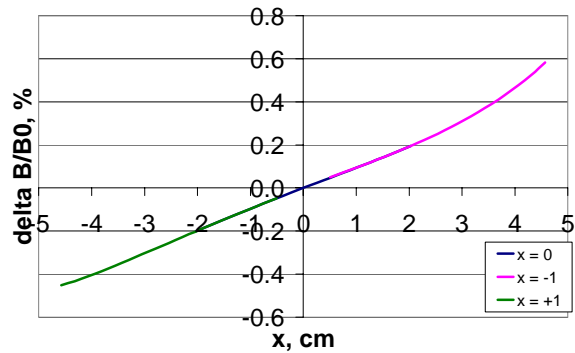


Figure 3 Fractional deviation from the central value of the $\int B_y dl$ recreated from rotating coil measurements at three different x positions, $x = 0$ cm, $x = -2.54$ cm, $x = +2.54$ cm.

AC Measurements

The power supply for the AC field measurement is a half-sine wave pulser that provides an output at the nominal peak current of 15 kA. It was not possible to excite the magnet with a flat-top pulse similar to the actual operational current for these measurements.

The measurements were taken using a long single turn Bdot coil so that the total field integral is measured. The probe is scanned from side to side across the aperture to provide field data as a function of position. The data are recorded, typically using a 20 pulse average, for both the Bdot coil and the power supply current simultaneously, with a 2.5 Msample/sec, 16-bit digitizer. The Bdot signal is digitally integrated and the result is normalized to the nominal 15 kA current. Table 2 and Figure 4 show the results of the field measurements on the first production magnet. Extrapolation of the DC field components from measurements at 500 A, 1000 A, and 1700 A indicate that the field components measured at higher AC current are probably compatible with those measured with the 1700 A DC current. The measured DC components are listed in Table 2 also.

Table 2: Field Components @ 25.4 mm

n	AC Measurements	DC Measurements
	@ 15 kAmps B_n/B_0	@ 1700 Amps B_n/B_0
0	1.0	1.0
1	1.435 e-3	2.40 e-3
2	4.782 e-5	-1.07 e-5
3	2.173 e-4	1.27 e-4
4	4.005 e-5	1.13 e-5
5	-2.000 e-5	-1.54 e-5
6	-2.297 e-5	-2.31 e-5

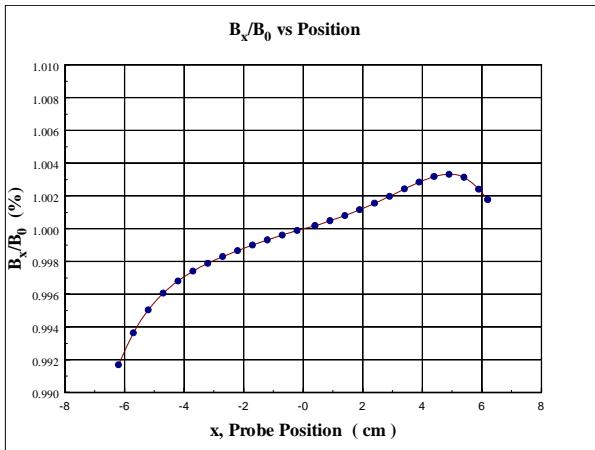


Figure 4 Field variation as a function of probe position. $\pm 1\%$ full scale.

DISCUSSION

Magnet modeling prior to production had predicted some amount of quadrupole component due primarily to asymmetric current flow at the power feed end of the magnet and an attempt was made to compensate this effect by modifying the shape (see Figure 1) of the crossover conductors. A small quadrupole component is not a concern if the magnet is used in a four-magnet injection scheme similar to the present injection method, since the magnets can be arranged to cause dipole fold-

down effects of the quadrupole components to cancel exactly. However, a new injection scheme [4] using only three bump magnets, has since been proposed and is going to be installed in the Booster. In this configuration the cancellation is not exact and will cause an orbit distortion of ± 2.5 mm while the bump magnet field ramps down at the end of the beam injection [5,6]. Various methods of compensation without rebuilding the magnet are being investigated. It is felt that this small orbit distortion will not be a significant problem even if it is left uncompensated.

REFERENCES

- [1] G4, National Magnetic Group, Inc.
1210 Win Drive, Bethlehem, Pennsylvania
18017- 7061 USA
Also available elsewhere as CMD10
- [2] PEEK™ Victrex®, Victrex plc, Victrex
Technology Centre, Hillhouse International,
Lancashire FY5 4QD
- [3] Vector Fields Limited, 24 Bankside, Kidlington,
Oxford, OX5 1JE, England
- [4] M.B. Popovic, A Proposed H- Injection System for
the Fermilab Booster, Beamdoc-1784, 2005.
- [5] E.J. Prebys, 2005, FNAL unpublished document.
- [6] A. Drozhdin, 2005, FNAL unpublished document.